INVERSE TRANSONIC AIRFOIL DESIGN

INCLUDING VISCOUS INTERACTION*

Leland A. Carlson
Texas A&M University

SUMMARY

A numerical technique has been developed for the analysis of specified transonic airfoils or for the design of airfoils having a prescribed pressure distribution, including the effect of weak viscous interaction. The method uses the full potential equation, a stretched Cartesian coordinate system, and the Nash-Macdonald turbulent boundary layer method. Comparisons with experimental data for typical transonic airfoils show excellent agreement. An example shows the application of the method to design a thick aft-cambered airfoil, and the effects of viscous interaction on its performance are discussed.

INTRODUCTION

A numerical method for the design or analysis of transonic airfoils should not only be accurate but also should be as simple as possible in concept and approach. It should use coordinate systems, input variables, and boundary condition treatments that can be easily understood by the user. Finally, it should be able to handle both shocked and shockless flows and be suitable not only for complete design but also for airfoil modification.

One approach to this problem is the inverse method in which the airfoil surface pressure is specified and the airfoil shape subsequently determined. Admittedly, this approach requires knowledge of what would be a desirable pressure distribution, but this characteristic is probably understood by the designer as well as any other. Furthermore, the designer can select a pressure distribution that will approximate a desired lift and moment, have a reasonable supersonic zone, yield desirable boundary layer properties, and satisfy other transonic flow criteria.

The purpose of this paper is to present results obtained with a numerical method that is suitable for the analysis, design, or modification of subsonic and transonic airfoils. The method is similar to that of references 1-3, but it has been modified to include the effects of weak viscous interaction.

SYMBOLS

C_D drag coefficient

C_L lift coefficient

C_M pitching moment coefficient

*Partially supported by NASA Grant NSG1174.

C_p pressure coefficient

c chord

M_∞ free stream Mach number

RN Reynolds number

w weighting factor

α angle of attack

δ^* boundary layer displacement thickness

PROBLEM FORMULATION

To solve the inviscid part of the flowfield, the method uses the exact equation for the perturbation potential in Cartesian coordinates. In order to avoid at supersonic points difficulties associated with nonalignment of the coordinates and the flowfield, a rotated finite difference scheme (ref. 4) is used in the solution; and in the actual program the infinite physical plane is mapped to a rectangular computational box. The resulting transformed finite difference equations are solved iteratively by column relaxation sweeping from upstream to downstream.

In the design mode, the shape of the nose region (typically 6-10% chord) is specified and a pressure distribution is prescribed over the remainder of the airfoil. Thus, the appropriate airfoil boundary condition in the direct region near the leading edge is the surface tangency requirement and in the inverse region, where the pressure is specified, it is essentially the specification of the derivative of the perturbation potential in the x-direction. In order to satisfy these at the airfoil boundary, which in general will not coincide with the Cartesian grid points, the derivatives in the boundary conditions are expanded as two term Taylor series about dummy points inside the airfoil. The derivatives in these series are then written in finite difference form using second order formulas for all first derivatives and at least first order ones for higher derivatives. In the direct region, central differences are used for x-derivatives and forward (on the upper surface) for the y-derivatives. However, to prevent numerical instability, the inverse region uses a second order backward difference formula for the first term of the Taylor series representing the x-derivative.

In the inverse case the airfoil must also be computed by integrating the surface tangency condition for the ordinates, y, as a function of x, with the initial conditions given by the slope and surface ordinate at the interface between the direct and inverse regions. In the present method, the latter are known because the nose region is solved directly, and the integration is accomplished using the Runge-Kutta method of order four.

It is believed, based on comparison with other results (ref. 3), that this method is an accurate and numerically consistent approach to the design and

analysis of transonic airfoils in inviscid flow. For further details concerning the finite difference, boundary condition, formulations, etc., see references 1 and 2.

BOUNDARY LAYER ANALYSIS

Experimental evidence (ref. 5-6) indicates that viscous boundary layer effects are very important in transonic flow. For example, the difference between the actual airfoil surface and the effective surface, i.e. the displacement surface, can cause an airfoil inviscidly designed to have a lift coefficient of 0.6 to actually develop 25%-50% less lift. To prevent such discrepancies, the effect of the boundary layer displacement thickness, δ^*, should be included in both the analysis and design portions of any numerical method.

In the present approach, the basic idea in the design case is to treat the airfoil determined by the inverse method as the displacement surface and to subtract from it the displacement thickness determined by a boundary layer computation. The result should be the actual airfoil ordinates. For the analysis case, the approach is to calculate a boundary layer displacement thickness and to use it to correct the location of the displacement surface (i.e. airfoil ordinate plus δ^*). The inviscid flowfield is then solved as before (ref. 1), where at present the displacement surface is updated every ten relaxation cycles.

Obviously the boundary layer scheme must be efficient, reliable, and accurate. Thus, three integral methods were considered for inclusion in the present numerical method—Walz Method II (ref. 7), the Nash-Macdonald method with smoothing (ref. 8-9), and Green's lag-entrainment method (ref. 10). Figure 1 compares for a typical transonic case the upper surface displacement thickness predictions from these methods with those obtained by Bavitz (ref. 11), who used the Bradshaw scheme (ref. 12) modified with a trailing edge correction. (The Walz results are not plotted but are between the Bradshaw and Nash-Macdonald data.) Notice that the predictions are essentially identical over most of the airfoil, and all but Green's method predict separation near the trailing edge. Apparently Green's method needs some type of trailing edge correction. Since the Walz and Green methods numerically fail at separation due to their empirical equations and since the Nash-Macdonald approach is 3-6 times faster, it was selected for incorporation into the present transonic airfoil design-analysis program.

ANALYSIS RESULTS

To start the direct problem the airfoil shape is inputed and a cubic spline fit and used to determine the ordinates and slopes in the computational plane. Next, to get some reasonable perturbation potentials, fifty relaxation cycles are performed on a very coarse grid (typically 13 x 7). Then the grid spacing is halved to a coarse grid (25 x 13) and fifty more cycles computed. At that point δ^* is computed and the displacement surface ordinates updated using under relaxation, i.e. $\delta^*_{new} = \delta^*_{old} + w(\delta^* - \delta^*_{old})$. The slopes are then determined from cubic splines through the new ordinates. The ordinates are updated every ten cycles thereafter. Typically, 400 cycles are performed on the coarse grid before halving to the medium grid (49 x 25), where 200-250 cycles are carried out. While this grid yields 66 points on the airfoil, the

grid may be, if desired, halved again (to 97 x 49) to obtain 130 points on the airfoil. Compared to inviscid cases, convergence on the fine grid is slow, and 400 relaxation cycles may be required. Fortunately, in many cases accurate results can be obtained on the medium grid. However, if double shocks exist, the fine grid may be needed to resolve them accurately. Convergence is determined by monitoring the changes in perturbation potential and δ^*.

Typical total computation times on an Amdahl 470/V6 are one minute for medium grid results and less than 4 minutes for fine grid data (about 10 minutes on a CDC 6600). Convergence is usually faster on CDC type machines due to the increase in significant digits.

As shown on figure 2, the present method can be used to demonstrate the effects of viscous interaction on a Korn 75-06-12 airfoil (ref. 9) near its design point. While the primary effect of the boundary layer is a 25% decrease in lift from the inviscid design value due to the pressure change on the upper surface, the lower surface pressure distribution is also affected. In addition, notice the excellent agreement between the viscous theory predictions and NAE wind tunnel data (ref. 6).

Another comparison with experimental data is shown on figure 3, again for the Korn airfoil but at an off-design condition. Although the minimum peak pressure and shock jump are slightly in error, which is not surprising since the method uses nonconservative finite differences, the overall agreement is excellent. Other results are shown in Table I, which compares data obtained with the present theory with experimental values at about the same lift. Many of these were obtained using the medium grid results only, and it is believed that they indicate that the present viscous analysis method is adequate for engineering studies of lift, drag, and moment variation. This is particularly true when the large discrepencies between viscous and inviscid results and the small differences between viscous results and experiments are considered.

DESIGN RESULTS

The computational procedure used in the inverse case is the same as described in references 2 and 3 except that δ^* is subtracted from the displacement surface. The final design is usually obtained on the medium grid after 250 relaxation cycles, although strong aft-cambered cases may require 400. At present there are some minor difficulties, due to the use of backward differences on the pressure boundary condition, in obtaining a desired pressure distribution near the trailing edge; and thus, the possibility of using the fine grid in design is under study. At present, a typical inverse run takes about 70 seconds (Amdahl 470/V6). It should be noted that in obtaining the actual airfoil ordinates a transition point must be selected, and the final shape is somewhat sensitive to this choice.

The importance of including the boundary layer in the design process is shown on figure 4. The shockless pressure distribution (solid line) used for this typical inverse design yielded for this Mach 0.72 case a 16% thick, highly aft-loaded airfoil. If the displacement surface ordinates were to be used to fabricate the airfoil instead of the correct values (i.e. if the boundary layer were ignored), the actual pressure distribution would be as shown by the

symbols. This result, which was obtained using the present viscous analysis method, shows a lift and moment 20% less than the design values.

On the other hand, when δ^* is included in determining the ordinates and the resultant airfoil is analyzed with viscous effects included, the agreement is much better. The medium grid results for this case are shown on figure 5. Here, transition is assumed to occur just aft of the minimum peak pressure; and the δ^* computed for the design pressure distribution differs by less than 0.013% from the δ^* determined in the analysis calculation. Nevertheless, as can be seen on figure 5, there is still a slight difference in the pressure distributions. However, considering the accuracy of boundary layer computations, sensitivity to transition location, and the large difference between viscous and inviscid results, the agreement is quite good. In addition, it indicates acceptable numerical consistency between the present analysis and design techniques.

CONCLUSION

Based upon experimental comparisons, it is believed that the present viscous analysis method is suitable for obtaining engineering estimates of the characteristics of transonic airfoils. In addition, while the inverse design method has not been verified, it has been shown to be numerically consistent with the analysis results at the medium grid level. Efforts to extend the design procedure to a fine grid are in progress and will be reported later.

REFERENCES

1. Carlson, L.A.: Transonic Airfoil Flowfield Analysis Using Cartesian Coordinates. NASA CR-2577, August 1975.
2. Carlson, L.A.: Transonic Airfoil Design Using Cartesian Coordinates. NASA CR-2578, April 1976.
3. Carlson, L.A.: Transonic Airfoil Analysis and Design Using Cartesian Coordinates. Proc. AIAA 2nd Computational Fluid Dynamics Conference, June 19-20, 1975, pp. 175-183.
4. South, J.Jr.; and Jameson, A.: Relaxation Solutions for Inviscid Axisymmetric Transonic Flow over Blunt or Pointed Bodies. Proc. AIAA Computational Fluid Dynamics Conference, July 1973, pp. 8-17.
5. Melnik, R.E.; and Ives, D.C.: On Viscous and Wind-Tunnel Wall Effects in Transonic Flows over Airfoils. AIAA Paper 73-660, July 1973.
6. Kacprzynski, J.J.: An Experimental Analysis and Buffet Investigation of the Shockless Lifting Airfoil No. 1. LR-569(NRC No. 13673), Nat. Res. Council Canada (Ottawa), August 1973.
7. Walz, A.: Boundary Layers of Flow and Temperature. MIT Press, Cambridge, Mass., 1969.
8. Nash, J.F.; and Macdonald, A.G.J.: The Calculation of Momentum Thickness in a Turbulent Boundary Layer at Mach Numbers up to Unity. Aero. Res. Council, C.P. No. 963, 1967.
9. Bauer, R., Garabedian, P., Korn, D.; and Jameson, A.: Supercritical Wing Sections II. Springer-Verlag, New York, 1975.
10. Green, J.E., Weeks, D.J.; and Brooman, J.W.F.: Prediction of Turbulent Boundary Layers and Wakes in Compressible Flow by a Lag-Entrainment Method. RAE Tech. Report TR-72231, January 1973.

11. Bavitz, P.C.: An Analysis Method for Two-Dimensional Transonic Viscous Flow. NASA TN D-7718, January 1975.
12. Bradshaw, P.; and Ferriss, D.H.: Calculation of Boundary Layer Development Using the Turbulent Energy Equation: Compressible Flow on Adiabatic Walls. Journal Fluid Mech., Vol. 46, pt. 1, March 1971.

Table I.- COMPARISON WITH EXPERIMENT

	M_∞	C_D Theory	C_D Expt	C_D Theory	C_D Expt	C_D Theory	C_D Expt
1	.622	.48	.49	-.105	-.104	.0070	.0070
2	.699	.667	.667	-.107	-.106	.0108	.0107
3	.75	-.097	-.093	-.111	-.114	.0209	.0146
4	.75	.104	.100	-.118	-.126	.0086	.0092
5	.75	.454	.458	-.120	-.121	.0086	.0090
6	.75	.516	.515	-.122	-.121	.0089	.0086
7	.75	.523	.523	-.119	-.120	.0092	.0094
8	.75	.539	.535	-.122	-.120	.0095	.0088
9	.75	.601	.597	-.119	-.122	.0110	.0081
10	.75	.711	.712	-.130	-.125	.0151	.0125
11	.15	.475	.47	-.099	-.105	.0085	.009

Note: Cases 1-11, 75-06-12 at RN=21 x 10^6, Case 11 GA(W)-2 at 6 x 10^6

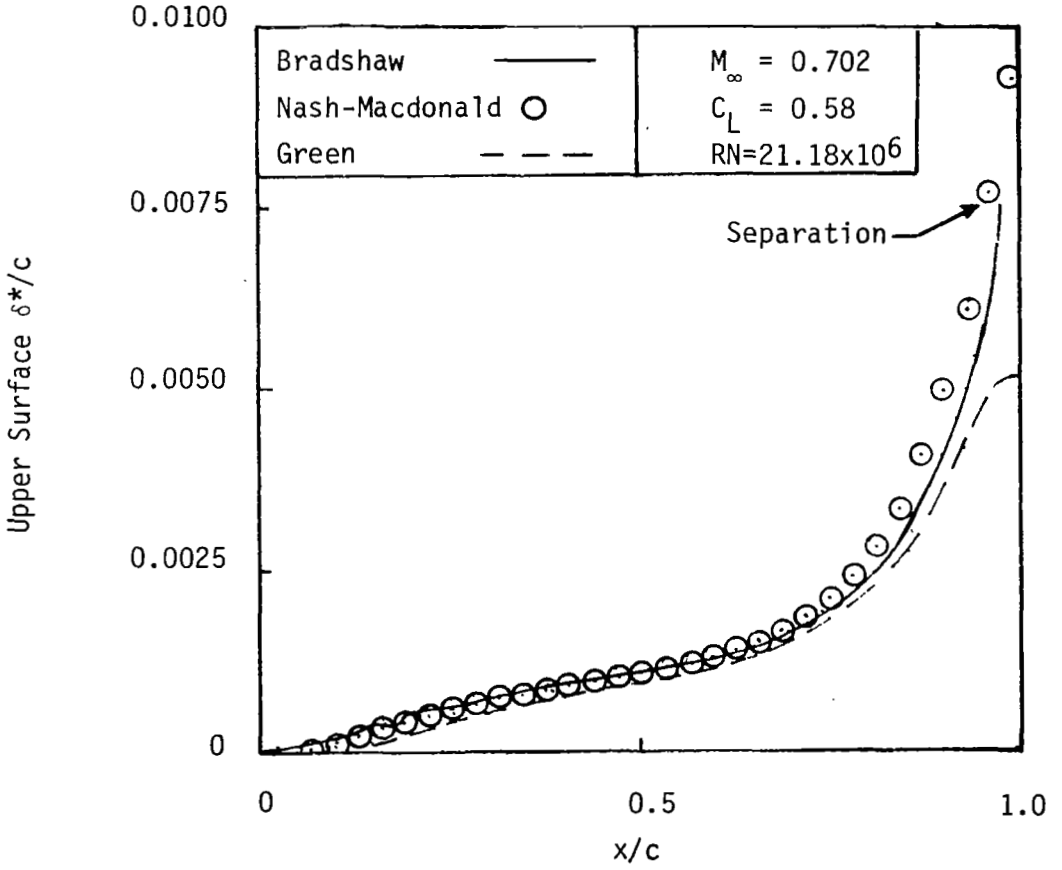

Figure 1.- Comparison of boundary layer results for Korn airfoil 75-06-12.

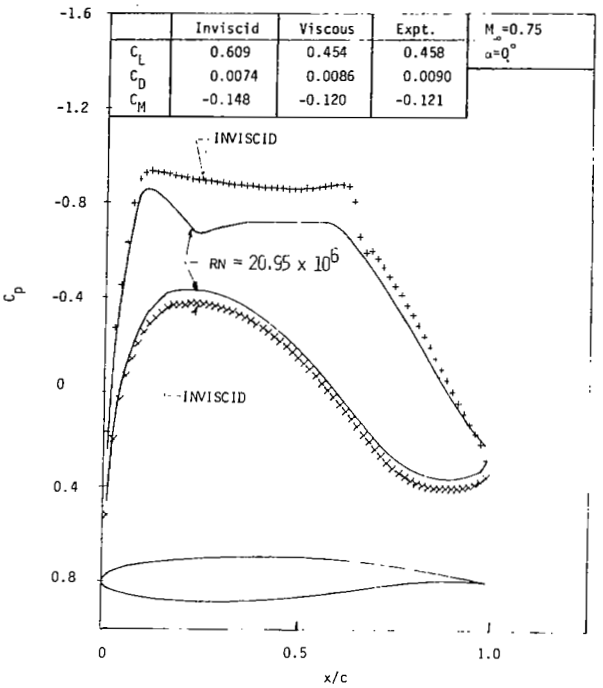

Figure 2.- The effect of viscous interaction of the Korn airfoil 75-06-12.

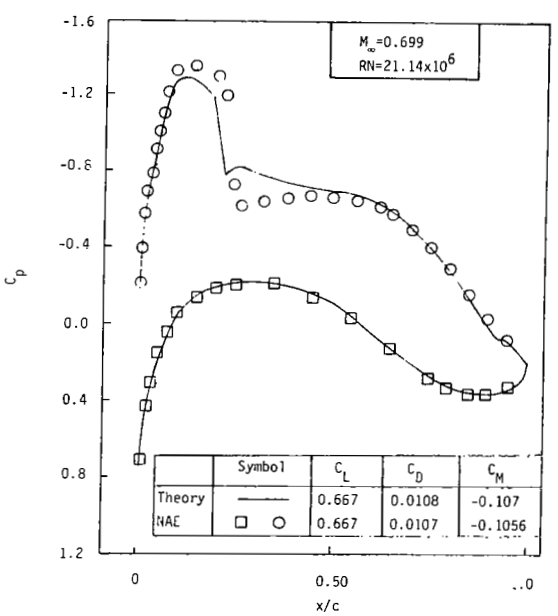

Figure 3.- Comparison of NAE data with present results.

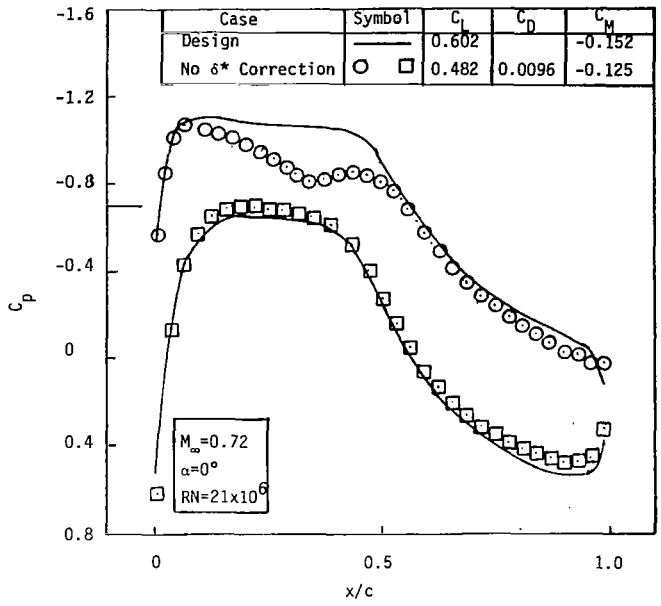

Figure 4.- Comparison of design predictions with results for airfoil fabricated without boundary layer correction.

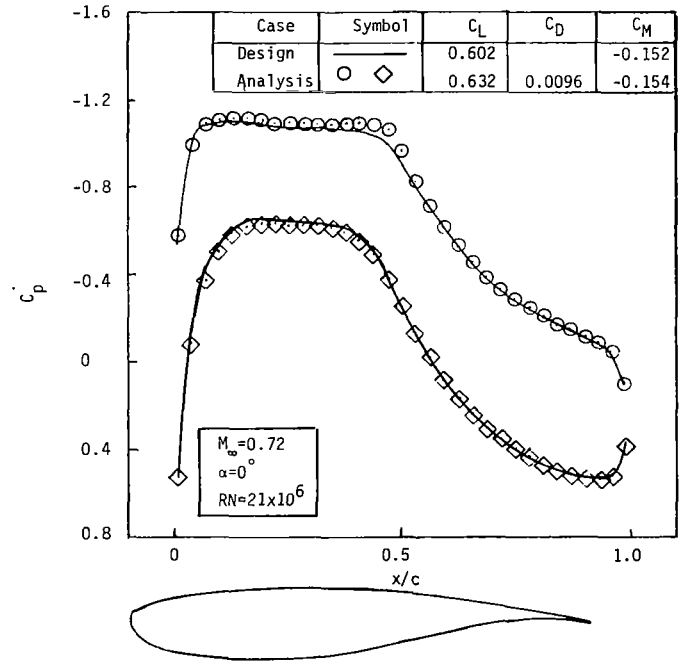

Figure 5.- Comparison of design predictions with viscous analysis results.